HHS Public Access

Author manuscript

ACS Chem Neurosci. Author manuscript; available in PMC 2018 May 03.

Published in final edited form as:

ACS Chem Neurosci. 2017 May 17; 8(5): 1053–1064. doi:10.1021/acschemneuro.7b00020.

Specific Connectivity and Unique Molecular Identity of MET Receptor Tyrosine Kinase-Expressing Serotonergic Neurons in the Caudal Dorsal Raphe Nuclei

Ryan J. Kast[1,2,4], **Hsiao-Huei Wu**[2,4], **Piper Williams**[2], **Patricia Gaspar**[3], and **Pat Levitt**[1,2,*]

[1]Neuroscience Graduate Program, University of Southern California, Los Angeles, CA

[2]Department of Pediatrics and the Institute for the Developing Mind, The Saban Research Institute, Children's Hospital Los Angeles, Keck School of Medicine, University of Southern California, Los Angeles, CA

[3]Inserm, UMRS-839, Université Pierre et Marie Curie, and Institut du Fer à Moulin, Paris, France

Abstract

Molecular characterization of neurons across brain regions has revealed new taxonomies for understanding functional diversity even among classically defined neuronal populations. Neuronal diversity has become evident within the brain serotonin (5-HT) system, which is far more complex than previously appreciated. However, until now it has been difficult to define subpopulations of 5-HT neurons based on molecular phenotypes. We demonstrate that the MET receptor tyrosine kinase (MET) is specifically expressed in a subset of 5-HT neurons within the caudal part of the dorsal raphe nuclei (DRC) that is encompassed by the classic B6 serotonin cell group. Mapping from embryonic day 16 through adulthood reveals that MET is expressed almost exclusively in the DRC as a condensed, paired nucleus, with an additional sparse set of MET+ neurons scattered within the median raphe. Retrograde tracing experiments reveal that MET-expressing 5-HT neurons provide substantial serotonergic input to the ventricular/subventricular region that contains forebrain stem cells, but do not innervate the dorsal hippocampus or entorhinal cortex. Conditional anterograde tracing experiments show that 5-HT neurons in the DRC/B6 target additional forebrain structures such as the medial and lateral septum and the ventral hippocampus. Molecular neuroanatomical analysis identifies fourteen genes that are enriched in DRC neurons, including 4 neurotransmitter/neuropeptide receptors and 2 potassium channels. These analyses will lead to future studies determining the specific roles that 5-HT^{MET+} neurons contribute to the broader set of functions regulated by the serotonergic system.

Keywords

serotonin; B6; Dorsal Raphe; neurodevelopment; Stem Cells; Autism

Correspondence to: Pat Levitt, Ph.D., The Saban Research Institute, Children's Hospital Los Angeles, 4650 Sunset Blvd., Los Angeles, CA90027, plevitt@usc.edu.

[4]These authors contributed equally for this work

Supporting Information

The supporting information document contains four supplemental figures and one supplemental table, including figure captions for each item.

Introduction

Serotonergic neurons in the rodent brainstem were mapped in detail in a series of studies more than 50 years ago[1,2,3]. Since then, many efforts have been made to characterize the topographical and functional organization of serotonergic systems[4,5,6,7–9]. Using a variety of methods, the raphe complex was originally delineated into caudal (B1–B3), median (B5 and B8), and dorsal (B6 and B7) raphe nuclei[4–6,3,7,8]. More recently, the raphe complex has been subcategorized into ventral (DRV), dorsal (DRD), and ventrolateral (DRVL) compartments, which collectively form the B7 group, and the caudal (DRC) group, which corresponds to the classically defined B6 subgroup[9,10,11,12,13]. Serotonergic axons reach almost every portion of the neuraxis, motivating efforts to understand the molecular, functional, and physiological properties of the dorsal raphe nuclei (DRN) and median raphe nuclei (MRN). Subtypes of raphe 5-HT-containing neurons have been identified based on differential innervation patterns, electrophysiological characteristics and molecular profiles[14–17]. Additionally, It has been shown that subpopulations of DRN 5-HT neurons are differentially activated by stressful stimuli[12,18]. Recent developmental analysis has characterized the rhombomeric origins of specific raphe subnuclei and identified several transcription factors involved in their production and specification[19,20,21,22]. With increasing availability of molecular and genetic tools, knowledge of the developmental and functional diversity of 5-HT neurons is being advanced. For example, a recent intersectional genetic labeling strategy identified a specialized subset of molecularly-defined 5-HT neurons that mediates normal respiratory CO_2 chemoreflex[23]. Identifying additional molecular subtypes of 5-HT neurons, therefore, promises to improve our understanding of the serotonergic system.

In the developing mouse brain, we reported highly selective expression patterns[24,25] of the *Met* receptor tyrosine kinase (MET), an autism risk gene[26]. Through initial mapping, *Met* expression was discovered in a limited subset of raphe 5-HT neurons residing under the aqueduct in the DRC[25]. Evidence from studies in the forebrain revealed restricted expression of hepatocyte growth factor (HGF)[27], the only known ligand for the MET receptor, and that activation controls several aspects of cortical neuron maturation, including dendritic, axonal, and synaptic phenotypes[27,28]. Currently, there is limited understanding of the impact of MET signaling on the development and function of the 5-HT neurons that express MET (5-HT^{MET+}). A deficit in a social approach measure in *Met* conditional knockout animals was recently reported in experiments using a Cre line[15] driven by the promoter of the 5-HT neuron-specific ETS transcription factor *Pet1*[29,30], which results in recombination of alleles in the 5-HT neurons that express the conditionally floxed gene. Thus, 5-HT^{MET+} neurons may influence certain aspects of complex behaviors.

The discovery of a specific and highly circumscribed subpopulation of 5-HT^{MET+} neurons leads to questions to determine the detailed molecular and connectivity properties of these neurons, establishing a framework for detailed functional analyses. The present study characterizes the neuroanatomical and molecular phenotypes of 5-HT^{MET+} neurons, focusing on the small, compact group residing in the DRC. The results demonstrate novel phenotypes that distinguish these neurons from other 5-HT neurons in the DRN, thus

contributing to the concept that 5-HT^{MET+} neurons are a highly specific subpopulation of serotonergic neurons that underlie unique functions.

Results and Discussion

We reported previously that *Met* is expressed in a limited number of 5-HT neurons located directly beneath the cerebral aqueduct in the caudal-most DRN[25], that will be referred to in the present study as DRC according to the more recent categorization outlined by Paxinos and Franklin[31]. This region includes the r1DRd, r1DRv and r1DRw domains defined by Alonso et al[20]. The onset of Met expression in this cell group occurred at embryonic day 15 and persisted through postnatal day 4, the last age examined in our previous report. Recently, Okaty and colleagues reported a similar restricted distribution of *Met* expression in the DRC, and an additional *Met+* subset of median raphe neurons in adult mice[15]. The similarity of the *Met* expression pattern at embryonic stages and in adulthood suggests that the specificity of *Met* expression in the DRN is maintained across the lifespan.

To provide a more detailed understanding of *Met* expression by 5-HT neurons of the DRN, we examined the co-localization of transcripts encoding *Met* and the serotonin synthesis rate-limiting enzyme tryptophan hydroxylase 2 (*Tph2*) using multiplex fluorescent in situ hybridization (ML-FISH) in cryosections prepared from P14 and adult mice that included the DRD and DRV (Bregma level −4.6mm; DRC and DRI, Bregma level −5mm; MRN, Bregma Levels, -4.6 and -5mm) (Figure 1). Similar to the pattern we reported at earlier developmental stages, *Met* mRNA was expressed by a high percentage (82% ±1.5%) of the *Tph2* expressing neurons in the DRC (Figures 1B, D–D″). Additionally, *Met* mRNA was expressed by a more limited number (21% ±2.6%) of *Tph2* expressing neurons in the median raphe nuclei (MRN) (Figures 1B, E–E″). In contrast, the DRD and DRV contained few *Met*-expressing *Tph2*+ neurons (DRD, 0.9% ±0.4%; DRV, 2.1% ±1.4%) (Figures 1B, C–C″).

To complement the description of the 5-HT neurons that express *Met* (5-HT^{MET+}), a bacterial artificial chromosome developed by the GENSAT project was used to create a transgenic reporter mouse (Met^{GFP}) that expresses green fluorescent protein (GFP) under the control of the *Met* promoter. To validate the use of this reporter mouse for determining the specific 5-HT neuron subpopulations that express *Met*, ML-FISH was used to detect *Tph2*, *Met*, and *GFP* transcripts in the Met^{GFP} mice (Supplemental Figure 1). There was a high degree of co-expression of *Met* and *GFP* transcripts in *Tph2*-positive neurons in the DRN, as nearly all *Met*-expressing *Tph2*-positive neurons co-expressed *GFP* (93% ±1%), and nearly all *GFP*-expressing *Tph2*-positive neurons co-expressed *Met* (99% ±1%) (Supplemental Figure 1 G and H). In the MRN, about half of the *Met*-expressing neurons did not express *GFP* transcript (Supplemental Figure 1 H). The data indicate that in the DRN, GFP is a high-fidelity reporter of endogenous *Met* expression. We note that, for identifying 5-HT^{MET+} neurons in the MRN, the reporter has less fidelity, as approximately 60% (±8%) of *Met*-expressing *Tph2*-positive cells did not express detectable levels of *GFP* transcript in the MRN. Consistent with the distribution of *Met* transcript (Figure 1), immunocytochemical staining with antibodies against 5-HT and GFP on cryosections prepared from adult Met^{GFP} mice showed that 80% (±2.32) of 5-HT+ neurons located in the DRC co-express GFP

(Supplemental Figure 2). GFP was expressed in a scattered few DRD, DRV and MRN 5-HT neurons. In fact, we had to examine a large number of sections through the DRD and DRV because most lacked any GFP neurons. In contrast, Tph2- and 5-HT-expressing neurons were present in every section through these subnuclei. Of interest in the context of these findings are recent studies suggesting that the input and output connectivity of DRC is more similar to that of the MRN than to more rostral components of the DRN[13, 32]. These observations led the authors to postulate that the 5-HT neurons located in the DRC may be inappropriately categorized as part of the classically defined DRN. The present data indicating that there is a common molecular signature, defined by *Met* expression, between neurons situated in DRC and a subset of the neurons in MRN supports this notion. Furthermore, to our knowledge, *Met* is the first non-serotonergic gene identified that is expressed by DRC and MRN 5-HT neurons, but with very limited expression by other 5-HT raphe subnuclei.

Selective innervation of the subventricular zone by Met-expressing 5-HT neurons

A recent examination of the axonal projection patterns of subsets of serotonergic raphe neurons was accomplished by targeting small injections of an adeno associated virus (AAV) encoding a Cre-dependent GFP reporter into different subregions of the raphe complex of $Sert^{Cre}$ mice[13]. This study suggested that many forebrain and brainstem structures receive input from a limited subset of DRN neurons, whereas subgroups of raphe neurons have distinct projection patterns. Of particular interest to the current study, these experiments suggested that DRC provides serotonergic innervation to limited forebrain structures, including the hippocampus, lateral septum, various cortical regions (e.g. entorhinal cortex), and the subventricular zone (SVZ)[13].

We wondered if some of these forebrain projections might arise from, and perhaps be a defining feature of, the 5-HT^{MET+} neurons in DRC and MR. Retrograde tracing in adult Met^{GFP} mice was thus performed by injecting fluorescent retrobeads into several forebrain structures. Of particular interest was the serotonergic innervation of the SVZ, as most 5-HT neurons that project to the SVZ are positioned in the DRC/B6 and the MRN[33–35], and a recent study found that the proliferation of adult stem cells in the SVZ is sensitive to pharmacological manipulations of 5-HT receptor signaling[33]. Moreover, we recently discovered that the transcript encoding the ligand that activates the MET receptor, *Hgf*, is expressed heavily in the SVZ beginning at E16 and persisting through P14[25, 27], the latest age examined. Mapping of retrogradely-labeled $retrobead^{+}$ neurons following injection of tracer into the lateral ventricle of adult Met^{GFP} mice showed a dense cluster of retrobead-labeled neurons positioned in the DRC (Figure 2), with only sparse labeling of neurons in DRV and the rostral MRN (Supplemental Figure 3, and data not shown). Remarkably, 86% (±2%) of $retrobead^{+}$ neurons in the DRC expressed GFP (Figure 2G). In contrast, there was very sparse retrograde labeling of neurons in the DRV and the rostral MRN, yet even some of the retrobead-labeled neurons in these subnuclei expressed GFP (Supplemental Figure 3), which is remarkable given that such a limited number of the neurons in these regions expressed *Met* or *GFP* transcript (Figure 1E and Supplemental Figure 3). These results

demonstrate that a substantial proportion of the serotonergic innervation of the SVZ is derived from 5-HT^{MET+} neurons that are predominantly clustered in the DRC.

To determine whether Met-expressing neurons in the DRC project to additional forebrain structures previously shown to receive serotonergic input from this raphe subregion[13], we injected retrobeads into the entorhinal cortex and CA1 of the dorsal hippocampus in a separate cohort of adult Met^{GFP} mice. There was very limited retrograde labeling of entorhinal- and hippocampal-projecting neurons positioned within or immediately adjacent to the cluster of 5-HT^{MET+} neurons in the DRC (Figure 3). Moreover, none of the neurons projecting to entorhinal cortex or CA1 of the dorsal hippocampus expressed GFP, even when these neurons were positioned within the DRC (Figure 3). Together, these retrograde tracing results suggest that the 5-HT^{MET+} neurons are a primary source of the serotonergic innervation to the SVZ, but do not project to CA1 of dorsal hippocampus or entorhinal cortex. It is worth noting that several of the regions (medial/lateral septum, ventricular surface, and ventral hippocampus) that receive dense serotonergic innervation from DRC express *Hgf* at P14[27], indicating that forebrain regions in addition to SVZ may receive serotonergic input from 5-HT^{MET+} neurons. This will be determined in future mapping studies.

The results from these retrograde tracing experiments provide evidence that 5-HT^{MET+} neurons innervate a select subset of forebrain structures, but they do not exclude the possibility that these neurons form collateral projections to additional forebrain structures that were not analyzed - nor do they provide a comprehensive map of the forebrain territories innervated by 5-HT^{MET+} neurons. In a previous study[13], the serotonergic projections arising from DRC were deduced from a set of conditional anterograde tracing cases that included viral transduction of Sert^{Cre} neurons in both DRC and a small number of DRL and MRN neurons. To refine previous descriptions of DRC projection patterns, we analyzed 2 additional Sert^{Cre}-mediated conditional AAV injection cases (S174 and S175) in which viral transduction was limited to approximately 50 neurons located exclusively in the caudal-most portion of DRC (Bregma level −5.34mm). These Sert^{Cre}-mediated, GFP-labeled cells abutted the fourth ventricle, with only a small number of neurons displaced laterally or ventrally. All of the GFP-labeled neurons contained 5-HT (Fig 4A–A″), and their axons could be followed up to the frontal pole. Proximal to the injection sites, some labeled axons could be visualized along the fourth ventricle ependyma in the brainstem (Figure 4A), but there was more extensive labeling of ascending projections that coursed through the ventral tegmental gray matter (vTG) and medial aspect of the medial forebrain bundle (MFB). Extensive innervation was observed within the medial and lateral septum, and the abutting subventricular zone (SVZ) (Figure 4B–D). Additional innervation was observed in the ventral hippocampus, and in the retromamillary nucleus (Figure 4E–E″). There was limited Sert^{Cre}–mediated, GFP-labeled 5-HT axonal innervation in the lateral preoptic area, lateral hypothalamus, and in the dorsal hippocampus. In comparison to the previous report[13], no innervation was seen in the cerebral cortex, thalamus, olfactory bulb or medial amygdala. The more limited set of forebrain regions innervated in these 2 cases suggests that some of the forebrain 5-HT axons deduced in earlier cases may have arisen from 5-HT neurons positioned in MRN, and DRL, rather than DRC[13]. The transduction of some laterally and ventrally displaced neurons precludes explicit conclusions regarding the

extent of collateralization of 5-HT^{MET+} DRC neurons or their projections to other sites. However, the consistent labeling of structures such as the septum and ventral hippocampus in current and previous[13] conditional anterograde tracing experiments suggests that additional projections from these neurons likely exist. Future Cre-dependent viral tracing in Met^{Cre} mice will provide important clarification of the specific telencephalic brain regions, other than the SVZ, that receive serotonergic input from the 5-HT^{MET+} neurons.

Molecular Characteristics of Met+ B6 5-HT neurons

Neurons within the DRD and DRV subnuclei are a major source of forebrain serotonin and represent the largest collection of serotonergic neurons, thus being the primary focus of studies on the putative roles of serotonin in psychiatric disorders. In comparison, relatively few studies have explored the function of serotonergic neurons in the DRC. This may be due in part to the lack of clear cytoarchitectural differences between DRC and other divisions of the raphe, and the limited molecular markers that distinguish neurons in the DRN subnuclei. There is some functional data. For example, intracerebroventricular injection of corticotropin releasing hormone (CRH) or urocortin 2 leads to selective increases in cFos expression in subsets of 5-HT neurons, including a considerable number in the DRC [3637, 38]. A receptor for CRH, corticotropin releasing hormone receptor 2 (*Crhr2*), is expressed in the caudal DRN in rat[39]. We wondered whether *Crhr2* expression might be enriched in 5-HT^{MET+} neurons. We performed ML-FISH using probes for *Tph2, Met,* and *Crhr2*. We found many *Crhr2*-expressing 5-HT neurons throughout the DRN including DRD, DRV, DRC, and DRI (Figure 5). ML-FISH revealed co-expression of *Crhr2* and *Met* in neurons residing in the DRC (Figure 5A–A′). Interestingly, even though 5-HT^{MET+} neurons co-express *Crhr2*, those DRC 5-HT neurons that displayed more fluorescent labeling of *Crhr2* transcript did not express *Met* (Figure 5A′). This result suggested that molecular heterogeneity of 5-HT neurons exists even within the DRC subnucleus.

To further delineate the molecular signatures of serotonergic neurons in the DRC, including the 5-HT^{MET+} population, we searched for genes enriched in the region by examining the developmental mouse brain database (P4) created by the Allen Brain Institute[40]. We used two different analytical strategies. Our initial analysis consisted of a manual search of gene expression patterns from a curated list of functionally-related genes termed “Gene Classification”. We examined the expression patterns of all the genes in the following categories: potassium channel, sodium channel, ion channel activity, ion gated ion channel activity, anion channel, calcium channel, calcium mediated signaling, cyclic nucleotide gated ion channel, neurotransmitter secretion, and neurological system process. A second analysis was conducted using the “AGEA” search tool, which identifies genes enriched within specific brain regions and at specific developmental time points of interest[40]. Within AGEA, we manually identified the caudal DRN and searched for genes enriched in the region at P4 and P14. In addition, there are two potentially enriched caudal DRN-expressing genes related to neuronal activity, the Potassium Voltage-Gated Subfamily A Member 4 (*Kcna4*) and μ-opioid receptor (*Oprm1*)[4142]. Analysis of the expression patterns of these 2 transcripts in the adult mouse brain atlas confirmed their enrichment in the DRC[43]. Thus, in total, we identified fourteen genes with the potential for substantial enrichment in subpopulations of DRC neurons during development (Table 1).

We analyzed in more detail six of the genes (Table 1) that are likely to play a role in influencing neuronal activity and synaptic transmission[44, 45]. The expression of these six genes in the P14 mouse DRN using ML-FISH was examined (Figure 6A′, B′, C′). In agreement with the patterns observed in the developing mouse brain atlas[40], qualitative assessment of each of the six genes displayed more intense labeling in the DRC than in more rostral DRD and DRV (Figure 6). However, unlike *Met*, low levels of each of the six transcripts also were detected throughout DRD and DRV, but with an increasing rostral to caudal gradient. The six genes displayed a variable degree of expression enrichment in the 5-HT^{MET+} neurons, but none exhibited an expression pattern as specific as that of *Met*. Two of the genes, *Kcnd2* and *Kcna4*, displayed relatively dense labeling in the DRC, with far less labeling in non-serotonergic neurons surrounding the nucleus (Figure 6). Notably, the most intense fluorescent labeling for *Kcnd2* and *Kcna4* was exhibited by the 5-HT^{MET+} neurons in the DRC (Figure 6A′, B′, C′ insets).

The other four genes (*Tacr3*, *Oprm1*, *Chrm2*, and *Chrna7*) also exhibited caudal DRN enrichment, but the differential fluorescent labeling between neurons in the DRC and the surrounding non-serotonergic neurons was less pronounced (Figure 6C–C″, green arrows; and data not shown). As was noted for *Met*, none of the six genes included in our analysis were detected in previous RNAseq experiments[46] as differentially expressed by 5-HT+ cells in the DRD or DRV. Interestingly, four of the seven DRC-enriched genes (*Met, Oprm1*, *Chrm2*, and *Tacr3*) identified in our analysis were detected in MRN populations in the RNAseq experiments of Okaty and colleagues[46]. These results further support the notion that a subset of DRC and MRN 5-HT neurons share common features that distinguish them from the 5-HT neurons in DRD and DRV.

In summary, the molecular neuroanatomical analyses suggest that 5-HT^{MET+} neurons are poised to respond to afferent inputs in a unique fashion that sets them apart from more rostral DRN 5-HT neurons. Specifically, their distinct gene expression profile, which includes potassium channels, neurotransmitter and neuropeptide receptors, suggests that they may have different intrinsic functional properties compared to other DRN neurons[17]. The afferent input that shapes the activity profile of 5-HT^{MET+} neurons remains to be determined, but the distinct efferent innervation pattern revealed by the present tracing studies suggests that 5-HT^{MET+} neurons are likely an important part of the circuitry regulating VZ/SVZ-related functions. Interestingly, recent reports suggest that the serotonergic innervation of the SVZ may be important in regulating the proliferation of adult stem cells located in this region[33]. With new genetic tools, we are now assessing the 5-HT^{MET+} neurons connectome and the function of this unique circuitry.

Conclusions

Here, we report novel data that further characterizes 5-HT^{MET+} neurons, which represent a limited subset of serotonergic neurons that exhibit a restricted projection pattern and a distinct molecular signature. A unique combination of phenotypes sets these neurons apart from other serotonergic neurons in the DRN. To our knowledge, *Met* is the first gene shown to be expressed specifically by a DRN subnucleus within a well-delimited anatomical site. It is worth noting that even though 5-HT^{MET+} neurons are situated predominantly in DRC, a

small subset of scattered MRN 5-HT neurons also express *Met*. Intriguingly, even though these neurons are positioned in a different raphe subnucleus, the MRN 5-HT^{MET+} neurons exhibit certain features of DRC 5-HT^{MET+} neurons, such as their projection to the SVZ. The significance of MET signaling in mediating developmental and functional processes of these serotonergic neurons is not known. In the neocortex and hippocampus, MET signaling mediates dendritic and axonal growth, de novo synapse formation *in vitro*, and the timing of excitatory synapse maturation and intracortical synaptic strength in vivo [27, 47–49]. Whether MET plays a similar role in the development of DRC serotonergic neurons will be an important line of investigation to pursue. Additionally, given that *Met* expression can be detected in DRC 5-HT neurons in adulthood, it will be important to determine whether MET signaling influences the functional properties of mature 5-HT^{MET+} neurons. As changes in HGF concentration in the cerebrospinal fluid (CSF) have been associated with several pathophysiological conditions[50–52], there is potential translational relevance in determining how HGF impacts the function of the 5-HT^{MET+} neurons. In this context, it is particularly interesting that 5-HT^{MET+} neurons are well positioned to respond to CSF signals through their supraependymal axons in the SVZ. Toward the goal of investigating detailed function of the 5-HT^{MET+} DRC neurons, the a new Met^{Cre} line that we are producing will provide novel genetic access to these neurons.

Methods

Animals

Animal care and experimental procedures were performed in accordance with the Institutional Animal Care and Use Committee of the Saban Research Institute, Children's Hospital Los Angeles. Mice were housed at 22°C on a 13/11-hour light/dark cycle (lights on at 0600h/lights off at 1900h) with ad libitum access to a standard chow diet (PicoLab Rodent Diet 20, #5053, St. Louis, MO). For AAV virus tracing experiments, animal care and experimental procedures were performed in accordance with the standard ethical guidelines (European Community Guidelines and French Agriculture and Forestry Ministry Guidelines for Handling Animals decree 87849). The SERT^{cre} mice[53] used for virus tracing were maintained on a C57Bl/6J background and locally bred and maintained under standard laboratory conditions (22 ± 1 °C, 60 % relative humidity, 12–12 h. light– dark cycle, food and water ad libitum).

To generate MET^{EGFP} reporter mice, a BAC clone (BX139) from the GENSAT project at the Rockefeller University (http://www.ncbi.nlm.nih.gov/pubmed/14746997?dopt=Abstract), constructed by insertion of EGFP into *Met* gene upstream of the ATG start codon of *Met* on BAC clone RP23-173P9[54], was purchased from Children's Hospital Oakland Research Institute (known as CHORI). BX139 was injected into FVB fertilized eggs (Cyagen Biosciences Inc. CA). 5 Founders carrying BX139 transgene, determined by PCR for the presence of GFP, were obtained. The GFP positive F1s from each founder, crossed with C57Bl/6J (JAX), were obtained. To determine whether the expression of the GFP reporter recapitulated Met expression, the brains of the F1s carrying BX139 transgene (determined by PCR) from each founder were examined at postnatal day (P) 0 using immunostaining with primary antibodies directed toward GFP and MET. We found line 17

and line 18 had the highest expression of GFP with an overall expression pattern that coincided closely with the pattern of MET at this age. All subsequent analysis was done using line 18, designated as Met^{GFP}. Homozygous $Met^{GFP/GFP}$ were derived from F1 crossing and the copy number of GFP was determined using Taqman GFP Copy Number Assay (Thermo Life Technology). The characterization of GFP expression in other brain regions will be detailed elsewhere (A. Kamitakahara, J. Wu and P. Levitt, unpublished results; R. Kast and P. Levitt, unpublished observations)

Tissue Processing

Tissue for immunofluorescence staining was collected from mice at postnatal day (P) 14. Tissue samples from both male and female mice were collected and assessed for MET expression in the brainstem by immunostaining. We found no difference in the labeling density of MET protein, or the cellular pattern of MET^{GFP} expression between sexes. Mice were deeply anesthetized by intraperitoneal injection of ketamine/xylazine (100 mg/kg: 10 mg/kg, Henry Schein, Melville, NY) and perfused transcardially with 0.9% saline, followed by 4% paraformaldehyde (PFA, Sigma, St. Louis, MO) in 0.1M phosphate buffered saline (PBS, pH 7.4). Whole brains were dissected and post-fixed in 4% PFA in PBS, cryoprotected in graded sucrose (10%, 20%, and 30% sucrose in PBS, overnight at 4°C for each concentration), embedded in VWR Clear Frozen Section Compound (VWR, Radnor, PA), and frozen in liquid nitrogen vapor.

For in situ hybridization, fresh whole brains from P7, 14, and adult mice were dissected by rapidly frozen by submersion in ice-cold isopentane as described[44, 55].

Brain tissues harvested for AAV tracing were processed as described[13].

Immunostaining

20μm sections were cut using a cryostat, mounted onto Superfrost Plus microscope slides (VWR, Radnor, PA), and processed for immunostaining as described[25, 55]. Primary antibodies used were as follows: Chicken anti-Green Fluorescent Protein (anti-GFP) (Abcam Cat# ab13970), goat anti-HGF receptor (anti-MET) (R and D Systems Cat# AF527), and rabbit anti-serotonin (anti-5HT, Sigma). Secondary antibodies used were as follows: Alexa 647 AffiniPure $F(ab')_2$ Fragment Donkey Anti-Chicken IgG (Jackson ImmunoResearch Labs, Cat# 703-546-155), Biotin-SP-AffiniPure $F(ab')_2$ Fragment Donkey Anti-Goat IgG (Jackson ImmunoResearch Labs, Cat# 705-066-147), DyLight 549 Streptavidin (Jackson ImmunoResearch Labs, Cat#016-580-084), Alexa 647 Donkey anti-Rabbit IgG (Thermo Fisher Scientific Cat# A-31573).

Multiplex Fluorescent In Situ Hybridization (ML-FISH)

Fresh-frozen tissues were cryosectioned at 16-μm and stored at −80°C. Commercially available RNAscope Multiplex Fluorescent reagent kits and RNAscope probes were used for transcript detection (Advanced Cell Diagnostics, Hayward, CA) as described[55]. RNAscope probes used in this study were as follows: Met (Cat# 405301), Tph2 (Cat# 318691), GFP (Cat# 400281), Kcna4 (Cat# 405311), Kcnd2 (Cat# 452581), Oprm1 (Cat# 315841), Tacr3 (Cat# 481671), Chrna7 (Cat# 465161), Chrm2 (Cat# 412121), and Crhr2 (Cat# 413201).

Retrograde tracing with retrobeads

Adult (P60–90) Met^{GFP} reporter mice were anesthetized with vaporized isoflurane (5% induction, 1.5–2% maintenance) and stabilized in a Narishige SG-4N small animal head holder. Depth of anesthesia was measured by respiration rate, and mice were maintained at 37°C for the duration of the surgical procedure using a TCAT-2 temperature controller (Physitemp Instruments, Inc.). Through stereotaxic guidance, a picospritzer connected to a pulled glass pipette (20 μm inner diameter and 35 μm outer diameter) was used to inject 100–200 nl of green or red Retrobeads™ IX (Lumafluor Inc.) into the desired forebrain target (see supplemental information for injection sites and stereotaxic coordinates). The needle was left in place for 5 minutes following injection, and then retracted slowly to minimize contamination of unintended brain regions along the needle tract. To minimize discomfort, mice were given a subcutaneous injection of the non-steroidal anti-inflammatory drug (NSAID) ketoprofen (5 mg/kg) immediately before the surgery, and ibuprofen (0.2 mg/mL) was provided in the drinking water for the first 3 days following surgery. Fourteen days after the surgery, mice were transcardially perfused with 4% paraformaldehyde dissolved in phosphate buffered saline (PBS) and tissue was processed for immunohistochemical analysis as described above.

Imaging and Anatomical Terminology

Fluorescent Images were acquired as Z stacks using a Zeiss Axio Observer Inverted microscope fitted with a LSM700 confocal scanner through a 20x/0.8NA Plan-APOCHROMAT objective (Cellular Imaging Core at the Saban Research Institute at Children's Hospital Los Angeles) controlled by Zeiss Zen 2009 program. Figures were prepared digitally using Adobe Photoshop CS5.1 and Adobe Illustrator CS5.1 (Adobe Systems In., San Jose, CA). Brightfield images were taken using Leica DMI6000B inverted microscope equipped with a 10x objective and a color CCD camera (Cellular Imaging Core at the Saban Research Institute at Children's Hospital Los Angeles).

The classic definition of the serotonergic B6 subgroup of the Dorsal Raphe Nucleus[2, 3] has been carefully studied cyto- and genoarchitecturally[20]. For the analysis of *Met*, the GFP reporter, other gene expression patterns, and retrogradely and anterogradely labeled neurons, we utilize the Paxinos and Franklin[31] designations of the Dorsal Raphe Nuclei, including dorsal (DRD), ventral (DRV), caudal (DRC), and interfascicular (DRI) subdivisions. There are two important notes related to our use of the Paxinos terminology. First, neurons located in the ventrolateral part of the dorsal raphe (DRVL) were included in the quantification of the DRD (Figure 1A). Second, we reserve the use of the term DRI for reference to the caudal aspect of the DRI, as depicted in the line drawing in Figure 1A. Using Pet-1+ cells at postnatal day (P) 10, Alonso et al.[20] genoarchitecturally define this portion of the DRI as the r1DRv, which is located immediately ventral to the r1DRd (Paxinos, DRC). This subset of caudal 5-HT neurons forms a slender, ventral trail of cells (r1DRv) that extends along the midline just above and in between the medial longitudinal fasciculus (MLF). The Median Raphe Nuclei extend ventrally from their dorsal limit, which is marked by the decussation of the superior cerebellar peduncle at rostral levels, and by the ventral aspect of the MLF at caudal levels.

Anterograde tracing using recombinant adeno-associated virus

Anterograde tracing experiments were done using $Sert^{Cre/+}$ mice obtained by crossing $Sert^{cre}$ male mice with C57-bl6-J mice[56]. As previously described (Muzerelle et al. 2016) replication-defective adeno-associated viruses (AAV-CAG.LSL.EGFP) from Penn Core Vector (University of Pennsylvania, USA) were used to obtain conditional GFP expression in 5-HT raphe neurons. Adult mice (P60) were anesthetized with ketamine (150 mg/kg)/ Xylazine (10 mg/kg), placed in a stereotaxic frame and 30 nl of AAV2/1/red fluorescent beads (7/1 v/v) was injected with a glass capillary pipet (40 μm tip diameter;) at the following coordinates from the Bregma (+ 5,35 AP, 0,5 L, 4,2 Deep), and 3 weeks after surgery mice were euthanized and transcardially perfused with buffered 4% paraformaldehyde. Brains were post-fixed overnight, cryoprotected in 30% sucrose and serially cut at 50μm on a sliding microtome (Microm Microtech, France). Free-floating sections were washed in PBS and incubated in a solution containing 1/1000 chick anti-GFP (Aves Labs), 1/5000 goat anti-Sert (Santa Cruz), or 1/3000 rabbit anti-5-HT (Sigma). Primary antibodies were applied 48 hrs at 4°C, sections washed extensively, and secondary antibodies (donkey-anti-chick-Alexa 488, Cy3-donkey antigoat, Cy5-donkey anti rabbit, all from Jackson laboratories) were applied for 2–4 hrs at room temperature. DAB-peroxidase immunostaining of GFP was performed on one complete series of sections[13]. Fluorescent images were acquired on a Leica SP5 confocal system, equipped with an Argon laser (for the 488nm excitation), a Diode 561 nm and HeNe 633nm. Z- series stacks of confocal images were acquired at 1024 × 1024 pixel resolution, with a pinhole set to one Airy unit and optimal settings for gain and offset. Mapping of GFP-expressing somata and axons were analyzed with a 40X/1.25 N.A Plan-apochromat.

Quantitative Image Analysis

IMARIS software (8.4.1) from Bitplane was used to quantify the percentage colocalization for each of the RNAscope ML-FISH and fluorescent immunocytochemistry experiments (including the retrograde tracing experiments). Specifically, three-dimensional renderings created from confocal z-stacks (images were collected within the anatomical location described in each figure and in the “Imaging and Anatomical Terminology” section of the methods section) were opened in IMARIS. Then, the spots tool was used to manually assign a spherical spot (dimeter =10μm) to each object (fluorescent signal resembling a cell) in each channel, while all other channels were hidden. Each successive channel was separately evaluated while the other channels were hidden. Once all objects had been separately identified in each fluorescent channel, the spots identified in separate channels were compared to identify cells that were positive for multiple fluorescent signals of interest.

For the ML-FISH experiments, the threshold for qualification as a positive cell was the presence of multiple fluorescent puncta/grains surrounding a DAPI-positive nucleus, with each punctum exhibiting fluorescence intensity qualitatively higher than background levels seen throughout the surrounding tissue. Similarly, for the retrograde tracing experiments, a retrograde positive cell was identified as any DAPI-positive nucleus surrounded by punctate fluorescent retrobeads. GFP-positive and 5-HT-positive cells labeled through immunocytochemical amplification were identified as smooth and continuous, cytosolic

signals, surrounding a DAPI-positive nucleus, and were each identified while all other fluorescent channels were hidden in the IMARIS display of the confocal z-stack.

Supplementary Material

Refer to Web version on PubMed Central for supplementary material.

Acknowledgments

We thank Aude Muzerelle for performing the surgery and histological processing for the AAV tracing study and Dr. Esteban Fernandez at the Cell Imaging Core of the Saban Research Institute for his excellent technical assistance. This work was supported by the Vanderbilt Conte Center for Neuroscience grant NIMH 5P50MH096972 (Project 2 and the Molecular Neuroanatomy core), NIMH R01 MH067842, and the Simms/Mann Chair in Developmental Neurogenetics to PL. RJK was supported by The Saban Research Institute Pre-Doctoral Research Career Development Fellowship. Work of PG was supported Investissements d'Avenir program (ANR-11-0004-02). The contents are solely the responsibility of the authors and do not necessarily represent the official views of the NIH. The authors declare no competing financial interests.

References

1. Dahlstrom AFK. Evidence for the existence of monoamine-containing neurons in the central nervous system. Acta Physiol Scand Suppl. 1964; 232:1–55.
2. Dahlström AFK. Localization of monoamines in the lower brain stem. Experientia. 1964; 20
3. Olson L, Seiger A. Early prenatal ontogeny of central monoamine neurons in the rat: fluorescence histochemical observations. Z Anat Entwickl Gesch. 1973; 137:301–316.
4. Azmitia EC, Segal M. An autoradiographic analysis of the differential ascending projections of the dorsal and median raphe nuclei in the rat. The Journal of comparative neurology. 1978; 179:641–667. [PubMed: 565370]
5. Vertes RP. A PHA-L analysis of ascending projectings of the dorsal raphe nucleus in the rat. J Comp Neurol. 1991; 313:643–668. [PubMed: 1783685]
6. Vertes RP, Fortin WJ, Crane AM. Projections of the median raphe nucleus in the rat. The Journal of comparative neurology. 1999; 407:555–582. [PubMed: 10235645]
7. Bobillier PSS, Degueurce A, Lewis BD, Pugol FJ. The efferent connections of the nucleus raphe centralis superior in the rat as revealed by radioautography. Brain Research. 1979:1–8.
8. Jacobs BL, Foote SL, Bloom FE. Differential projections of neurons within the dorsal raphe nucleus of the rat: a horseradish peroxidase (HRP) study. Brain Research. 1978; 147:149–153. [PubMed: 77700]
9. Vasudeva RK, Lin RC, Simpson KL, Waterhouse BD. Functional organization of the dorsal raphe efferent system with special consideration of nitrergic cell groups. J Chem Neuroanat. 2011; 41:281–293. [PubMed: 21640185]
10. Hale MW, Lowry CA. Functional topography of midbrain and pontine serotonergic systems: implications for synaptic regulation of serotonergic circuits. Psychopharmacology (Berl). 2011; 213:243–264. [PubMed: 21088958]
11. Hale MW, Shekhar A, Lowry CA. Stress-related serotonergic systems: implications for symptomatology of anxiety and affective disorders. Cell Mol Neurobiol. 2012; 32:695–708. [PubMed: 22484834]
12. Paul ED, Lowry Ca. Functional topography of serotonergic systems supports the Deakin/Graeff hypothesis of anxiety and affective disorders. Journal of Psychopharmacology. 2013; 27:1090–1106. [PubMed: 23704363]
13. Muzerelle A, Scotto-Lomassese S, Bernard JF, Soiza-Reilly M, Gaspar P. Conditional anterograde tracing reveals distinct targeting of individual serotonin cell groups (B5–B9) to the forebrain and brainstem. Brain Struct Funct. 2016; 221:535–561. [PubMed: 25403254]

14. Crawford LK, Craige CP, Beck SG. Increased intrinsic excitability of lateral wing serotonin neurons of the dorsal raphe: a mechanism for selective activation in stress circuits. J Neurophysiol. 2010; 103:2652–2663. [PubMed: 20237311]
15. Okaty BW, Freret ME, Rood BD, Brust RD, Hennessy ML, deBairos D, Kim JC, Cook MN, Dymecki SM. Multi-Scale Molecular Deconstruction of the Serotonin Neuron System. Neuron. 2015; 88:774–791. [PubMed: 26549332]
16. Kocsis BVV, Dahan L, Sik A. Serotonergic neuron diversity: Identification of raphe neurons with discharges time-locked to the hippocampal theta rhythm. Proceedings of the National Academy of Sciences. 2006
17. Fernandez SP, Cauli B, Cabezas C, Muzerelle A, Poncer JC, Gaspar P. Multiscale single-cell analysis reveals unique phenotypes of raphe 5-HT neurons projecting to the forebrain. Brain Struct Funct. 2016; 221:4007–4025. [PubMed: 26608830]
18. Hale MW, Shekhar A, Lowry CA. Stress-related serotonergic systems: Implications for symptomatology of anxiety and affective disorders. Cellular and Molecular Neurobiology. 2012; 32:695–708. [PubMed: 22484834]
19. Jensen P, Farago AF, Awatramani RB, Scott MM, Deneris ES, Dymecki SM. Redefining the serotonergic system by genetic lineage. Nat Neurosci. 2008; 11:417–419. [PubMed: 18344997]
20. Alonso A, Merchán P, Sandoval JE, Sánchez-Arrones L, Garcia-Cazorla A, Artuch R, Ferrán JL, Martínez-De-La-Torre M, Puelles L. Development of the serotonergic cells in murine raphe nuclei and their relations with rhombomeric domains. Brain Structure and Function. 2013; 218:1229–1277. [PubMed: 23052546]
21. Fox SR, Deneris ES. Engrailed is required in maturing serotonin neurons to regulate the cytoarchitecture and survival of the dorsal raphe nucleus. J Neurosci. 2012; 32:7832–7842. [PubMed: 22674259]
22. Simon HH, Scholz C, O'Leary DD. Engrailed genes control developmental fate of serotonergic and noradrenergic neurons in mid- and hindbrain in a gene dose-dependent manner. Mol Cell Neurosci. 2005; 28:96–105. [PubMed: 15607945]
23. Brust RD, Corcoran AE, Richerson GB, Nattie E, Dymecki SM. Functional and developmental identification of a molecular subtype of brain serotonergic neuron specialized to regulate breathing dynamics. Cell Rep. 2014; 9:2152–2165. [PubMed: 25497093]
24. Judson MC, Bergman MY, Campbell DB, Eagleson KL, Levitt P. Dynamic gene and protein expression patterns of the autism-associated met receptor tyrosine kinase in the developing mouse forebrain. J Comp Neurol. 2009; 513:511–531. [PubMed: 19226509]
25. Wu HH, Levitt P. Prenatal expression of MET receptor tyrosine kinase in the fetal mouse dorsal raphe nuclei and the visceral motor/sensory brainstem. Dev Neurosci. 2013; 35:1–16. [PubMed: 23548689]
26. Campbell DB, Sutcliffe JS, Ebert PJ, Militerni R, Bravaccio C, Trillo S, Elia M, Schneider C, Melmed R, Sacco R, Persico AM, Levitt P. A genetic variant that disrupts MET transcription is associated with autism. Proceedings of the National Academy of Sciences of the United States of America. 2006; 103:16834–16839. [PubMed: 17053076]
27. Eagleson KL, Lane CJ, McFadyen-Ketchum L, Solak S, Wu HH, Levitt P. Distinct intracellular signaling mediates C-MET regulation of dendritic growth and synaptogenesis. Dev Neurobiol. 2016; 76:1160–1181. [PubMed: 26818605]
28. Eagleson KL, Xie Z, Levitt P. The Pleiotropic MET Receptor Network: Circuit Development and the Neural-Medical Interface of Autism. Biol Psychiatry. 2017; 81:424–433. [PubMed: 27837921]
29. Hendricks TF, Nicole, Fyodorov Dmitry, Deneris ES. The ETS Domain Factor Pet-1 Is an Early and Precise Marker of Central Serotonin Neurons and Interacts with a Conserved Element in Serotonergic Genes. The Journal of Neuroscience. 1999; 19:10348–10356. [PubMed: 10575032]
30. Hendricks TF, DV, Wegman LJ, Lelutiu NB, Pehek EA, Yamamoto B, Silver J, Weeber EJ, Sweatt JD, Deneris ES. Pet-1 ETS Gene Plays a Critical Role in 5-HT Neuron Development and Is Required for Normal Anxiety-like and Aggressive Behavior. Neuron. 2003; 37:233–247. [PubMed: 12546819]
31. Paxinos, GF., KBG. The mouse brain in stereotaxic coordinates. 2. Academic Press; San Diego: 2001.

32. Commons KG. Ascending serotonin neuron diversity under two umbrellas. Brain Structure and Function. 2016:1–14.
33. Tong CK, Chen J, Cebrián-Silla A, Mirzadeh Z, Obernier K, Guinto CD, Tecott LH, García-Verdugo JM, Kriegstein A, Alvarez-Buylla A. Axonal control of the adult neural stem cell niche. Cell Stem Cell. 2014; 14:500–511. [PubMed: 24561083]
34. MIKKELSEN JDH-S, ANDERS, LARSEN PHILIPJ. Central Innervation of the Rat Ependyma and Subcommissural Organ With Special Reference to Ascending Serotoninergic Projections From the Raphe Nuclei. The Journal of Comparative Neurology. 1997:556–568. [PubMed: 9259489]
35. SIMPSON KLF, TODD M, WATERHOUSE BARRYD, LIN RCS. Projection Patterns From the Raphe Nuclear Complex to the Ependymal Wall of the Ventricular System in the Rat. The Journal of Comparative Neurology. 1998; 399:61–72. [PubMed: 9725701]
36. Hale MW, Stamper CE, Staub DR, Lowry CA. Urocortin 2 increases c-Fos expression in serotonergic neurons projecting to the ventricular/periventricular system. Experimental Neurology. 2010; 224:271–281. [PubMed: 20382145]
37. Staub DR, Spiga F, Lowry CA. Urocortin 2 increases c-Fos expression in topographically organized subpopulations of serotonergic neurons in the rat dorsal raphe nucleus. Brain Res. 2005; 1044:176–189. [PubMed: 15885216]
38. Staub DR, Evans AK, Lowry CA. Evidence supporting a role for corticotropin-releasing factor type 2 (CRF2) receptors in the regulation of subpopulations of serotonergic neurons. Brain Res. 2006; 1070:77–89. [PubMed: 16403469]
39. Van Pett K, Viau V, Bittencourt JC, Chan RKW, Li HY, Arias C, Prins GS, Perrin M, Vale W, Sawchenko PE. Distribution of mRNAs encoding CRF receptors in brain and pituitary of bat and mouse. Journal of Comparative Neurology. 2000; 428:191–212. [PubMed: 11064361]
40. Thompson CL, Ng L, Menon V, Martinez S, Lee CK, Glattfelder K, Sunkin SM, Henry A, Lau C, Dang C, Garcia-Lopez R, Martinez-Ferre A, Pombero A, Rubenstein JL, Wakeman WB, Hohmann J, Dee N, Sodt AJ, Young R, Smith K, Nguyen TN, Kidney J, Kuan L, Jeromin A, Kaykas A, Miller J, Page D, Orta G, Bernard A, Riley Z, Smith S, Wohnoutka P, Hawrylycz MJ, Puelles L, Jones AR. A high-resolution spatiotemporal atlas of gene expression of the developing mouse brain. Neuron. 2014; 83:309–323. [PubMed: 24952961]
41. Templin JS, Bang SJ, Soiza-Reilly M, Berde CB, Commons KG. Patterned expression of ion channel genes in mouse dorsal raphe nucleus determined with the Allen Mouse Brain Atlas. Brain Research. 2012; 1457:1–12. [PubMed: 22534482]
42. Gardon O, Faget L, Chu Sin Chung P, Matifas A, Massotte D, Kieffer BL. Expression of mu opioid receptor in dorsal diencephalic conduction system: New insights for the medial habenula. Neuroscience. 2014; 277:595–609. [PubMed: 25086313]
43. Lein ES, Hawrylycz MJ, Ao N, Ayres M, Bensinger A, Bernard A, Boe AF, Boguski MS, Brockway KS, Byrnes EJ, Chen L, Chen L, Chen TM, Chin MC, Chong J, Crook BE, Czaplinska A, Dang CN, Datta S, Dee NR, Desaki AL, Desta T, Diep E, Dolbeare TA, Donelan MJ, Dong HW, Dougherty JG, Duncan BJ, Ebbert AJ, Eichele G, Estin LK, Faber C, Facer BA, Fields R, Fischer SR, Fliss TP, Frensley C, Gates SN, Glattfelder KJ, Halverson KR, Hart MR, Hohmann JG, Howell MP, Jeung DP, Johnson RA, Karr PT, Kawal R, Kidney JM, Knapik RH, Kuan CL, Lake JH, Laramee AR, Larsen KD, Lau C, Lemon TA, Liang AJ, Liu Y, Luong LT, Michaels J, Morgan JJ, Morgan RJ, Mortrud MT, Mosqueda NF, Ng LL, Ng R, Orta GJ, Overly CC, Pak TH, Parry SE, Pathak SD, Pearson OC, Puchalski RB, Riley ZL, Rockett HR, Rowland SA, Royall JJ, Ruiz MJ, Sarno NR, Schaffnit K, Shapovalova NV, Sivisay T, Slaughterbeck CR, Smith SC, Smith KA, Smith BI, Sodt AJ, Stewart NN, Stumpf KR, Sunkin SM, Sutram M, Tam A, Teemer CD, Thaller C, Thompson CL, Varnam LR, Visel A, Whitlock RM, Wohnoutka PE, Wolkey CK, Wong VY, Wood M, Yaylaoglu MB, Young RC, Youngstrom BL, Yuan XF, Zhang B, Zwingman TA, Jones AR. Genome-wide atlas of gene expression in the adult mouse brain. Nature. 2007; 445:168–176. [PubMed: 17151600]
44. Ye R, Feldmeyer D, Jacob MH, Nedivi E, Quinlan Ma, Iwamoto H, Wu HH, Green NH, Jetter CS, McMahon DG, Veestra-VanderWeele J, Levitt P, Blakely RD. Physical Interactions and Functional Relationships of Neuroligin 2 and Midbrain Serotonin Transporters. Front Synaptic Neurosci. 2016; 7:1–17.

45. Carrasquillo Y, Nerbonne JM. IA Channels: Diverse Regulatory Mechanisms. The Neuroscientist: a review journal bringing neurobiology, neurology and psychiatry. 2014; 20:104–111.
46. Okaty BW, Freret ME, Rood BD, Brust RD, Hennessy ML, deBairos D, Kim JC, Cook MN, Dymecki SM. Multi-Scale Molecular Deconstruction of the Serotonin Neuron System. Neuron. 2015:1–18.
47. Qiu S, Anderson CT, Levitt P, Shepherd GM. Circuit-specific intracortical hyperconnectivity in mice with deletion of the autism-associated Met receptor tyrosine kinase. J Neurosci. 2011; 31:5855–5864. [PubMed: 21490227]
48. Qiu S, Lu Z, Levitt P. MET receptor tyrosine kinase controls dendritic complexity, spine morphogenesis, and glutamatergic synapse maturation in the hippocampus. J Neurosci. 2014; 34:16166–16179. [PubMed: 25471559]
49. Xie Z, Eagleson KL, Wu HH, Levitt P. Hepatocyte Growth Factor Modulates MET Receptor Tyrosine Kinase and beta-Catenin Functional Interactions to Enhance Synapse Formation. eNeuro. 2016; 3
50. Kern MA, Bamborschke S, Nekic M, Schubert D, Rydin C, Lindholm D, Schirmacher P. Concentrations of hepatocyte growth factor in cerebrospinal fluid under normal and different pathological conditions. Cytokine. 2001; 14:170–176. [PubMed: 11396995]
51. Vargas DL, Nascimbene C, Krishnan C, Zimmerman AW, Pardo CA. Neuroglial activation and neuroinflammation in the brain of patients with autism. Ann Neurol. 2005; 57:67–81. [PubMed: 15546155]
52. Tsuboi YKK, Akatsu H, Daikuhara Y, Yamada T. Hepatocyte growth factor in cerebrospinal fluid in neurologic disease. Acta Neurol Scand. 2002:99–103. [PubMed: 12100369]
53. Narboux-Neme N, Pavone LM, Avallone L, Zhuang X, Gaspar P. Serotonin transporter transgenic (SERTcre) mouse line reveals developmental targets of serotonin specific reuptake inhibitors (SSRIs). Neuropharmacology. 2008; 55:994–1005. [PubMed: 18789954]
54. Gong S, Kus L, Heintz N. Rapid bacterial artificial chromosome modification for large-scale mouse transgenesis. Nat Protoc. 2010; 5:1678–1696. [PubMed: 20885380]
55. Wu HH, Choi S, Levitt P. Differential patterning of genes involved in serotonin metabolism and transport in extra-embryonic tissues of the mouse. Placenta. 2016; 42:74–83. [PubMed: 27238716]
56. Zhuang X, Masson J, Gingrich JA, Rayport S, Hen R. Targeted gene expression in dopamine and serotonin neurons of the mouse brain. J Neurosci Methods. 2005; 143:27–32. [PubMed: 15763133]

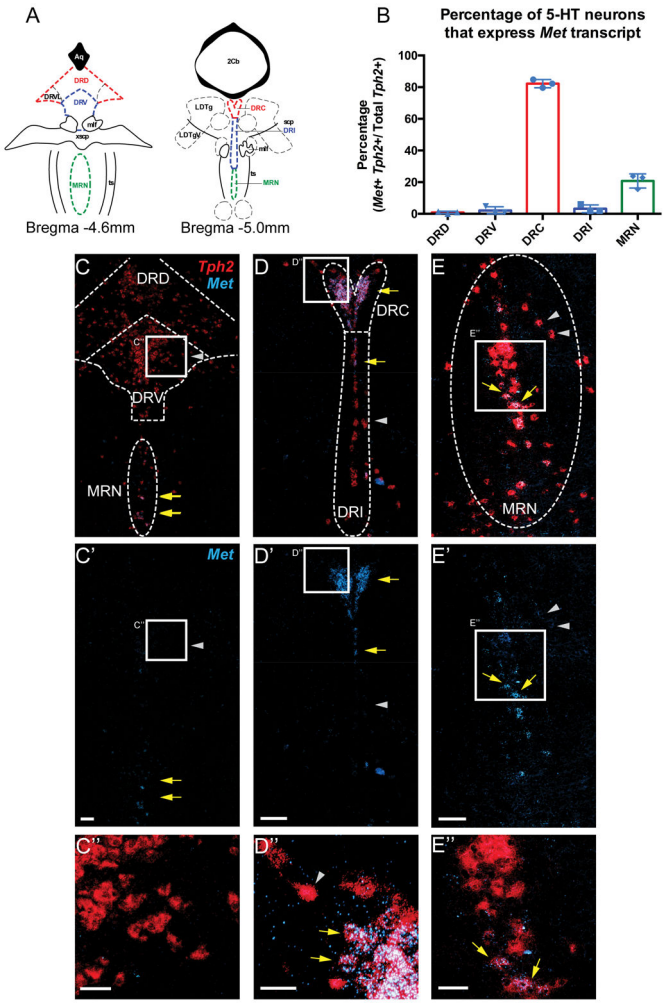

Figure 1. *Met* expression is enriched in 5-HT neurons positioned in the DRC

A) Line drawings modified from the Paxinos and Franklin[31] stereotaxic mouse brain atlas to illustrate the regions imaged and quantified in B–E″. B) Quantification (n = 3 mice) of the percentage of *Tph2*-positive neurons in each DRN subdivision that express *Met* transcript at postnatal day 14 (P14). C) Low magnification image of *Met* (light blue) and *Tph2* (red) transcripts detected by ML-FISH with RNAscope probes in cryosections containing the DRD, DRV, and rostral part of the MRN (Bregma level −4.6mm) prepared at P14. Yellow arrows indicate *Tph2*-positive cells that express *Met*. Gray arrowheads denote *Tph2*-positive cells that do not express *Met*. C′) Same image as C, with only *Met* signal shown. C″) High magnification image of region boxed in panel C. Note the absence of *Met* transcript from most *Tph2*-positive cells in the DRV. D) Low magnification image of *Met* and *Tph2* transcripts in the DRC and DRI subdivisions of the raphe (Bregma level −5.0 mm). D′) Same image as D, with only *Met* signal shown. D″) High magnification image of region boxed in panel D. Note the high degree of colocalization of *Met* and *Tph2* transcripts in the DRC. E) Low Magnification image of *Met* and *Tph2* transcripts in the MRN. E′) Same image as E, with only *Met* signal shown. E″) High magnification image of region boxed in panel E. Scale bars = 100 μm in C′, D′, and E′. Scale bars = 50 μm in C″, D″, and E″.

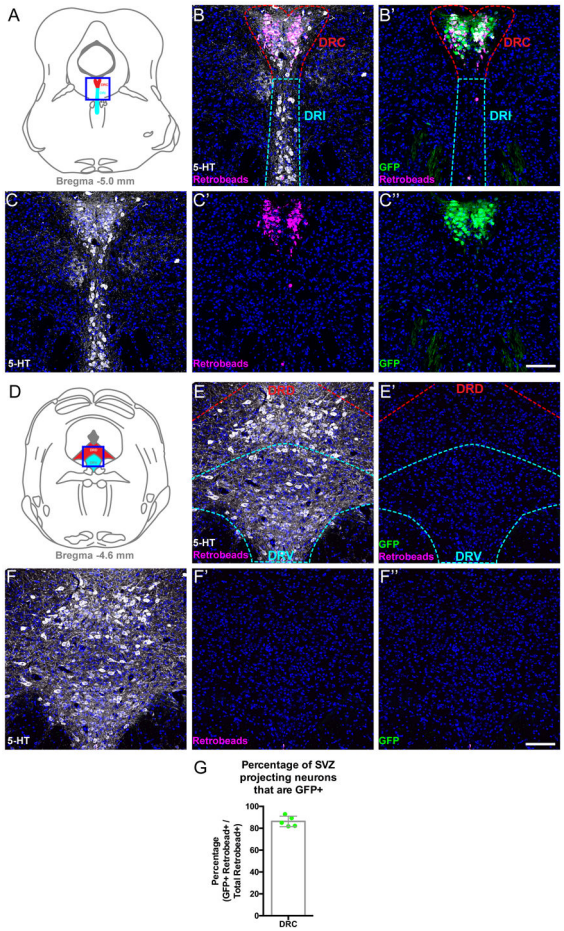

Figure 2. 5-HT^{MET+} neurons project to the subventricular zone of the lateral ventricle

A) Schematic line drawing modified from stereotaxic mouse brain atlas[31] to depict the region imaged (blue box) in B–C″ (Bregma level −5.0 mm). B) Coronal section through the DRC (red dashed line) and DRI (cyan dashed line) of the adult mouse brain. Section contains neurons retrogradely labeled from the lateral ventricle (magenta) and is immunolabeled with an anti-5-HT antibody (white). B′) The same region displayed in panel B, but immunolabeling with an anti-GFP (green) antibody is shown. C–C″) Split channels of images displayed in B and B′ (5-HT, white; retrobeads, magenta; GFP, green; DAPI, blue). D) Schematic line drawing depicting the region imaged (blue box) in E–F′ (Bregma level −4.6 mm). E) Coronal sections through the DRD (red dashed line) and DRV (cyan dashed line) immunolabeled with an anti-5-HT antibody (white). Notice the relative absence of SVZ-projecting neurons (magenta) at this level of the raphe complex. E′) The same coronal section as shown in panel E, but immunolabeling with an anti-GFP (green) antibody shown. F–F″) Split channels of images displayed in E and E′ (5-HT, white; retrobeads, magenta; GFP, green; DAPI, blue). G) Quantification of the percentage of SVZ-projecting neurons in the DRC that express GFP (n = 5 mice). Scale bars = 100 μm for all panels

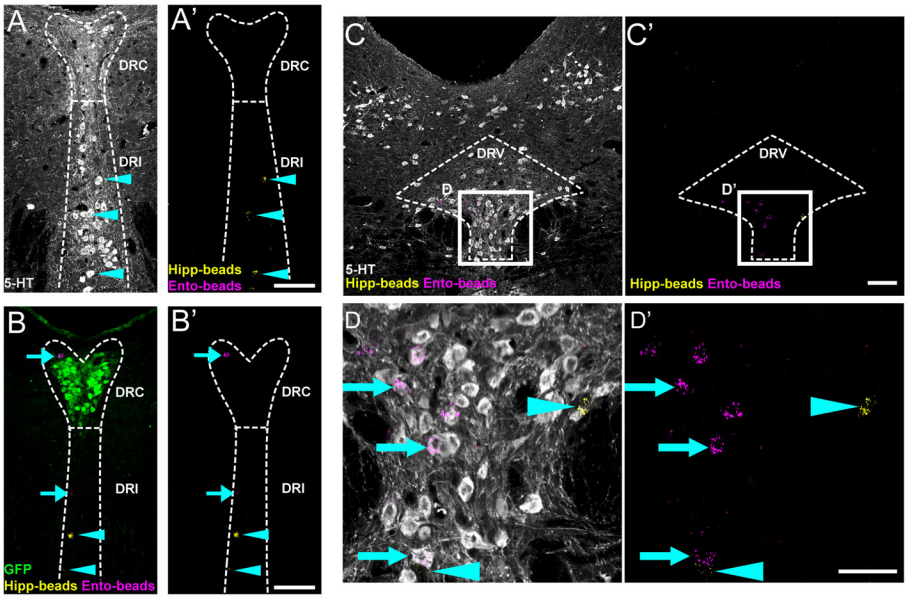

Figure 3. Dorsal raphe neurons that project to entorhinal cortex or dorsal hippocampus are distinct from 5-HT^{MET+} neurons

A–A′) Coronal section through the DRC and DRI (Bregma level – 5.2 mm) of adult Met^{GFP} brain. The section contains neurons retrogradely labeled from CA1 of dorsal hippocampus (yellow puncta, cyan arrowhead) that are positioned with the DRI. 5-HT immunolabeling (white) shows these hippocampal-projecting neurons are serotonergic. B–B′) Coronal section through the DRC and DRI (Bregma level −5 mm) containing entorhinal-projecting (magenta, cyan arrow) and hippocampal-projecting (yellow) neurons. GFP immunolabeling (green) indicates that the retrogradely labeled neurons are distinct from the 5-HT^{MET+} population, even when positioned within the DRC. C– C′) Coronal section through DRD and DRV (Bregma level −4.7 mm) containing entorhinal- and hippocampal-projecting neurons clustered in the DRV. 5-HT immunolabeling (white) shows that the entorhinal-projecting neurons are serotonergic. Neither population expresses GFP. D and D″) High magnification images of regions boxed in panels C and C″. Scale bars =100 μm for all panels.

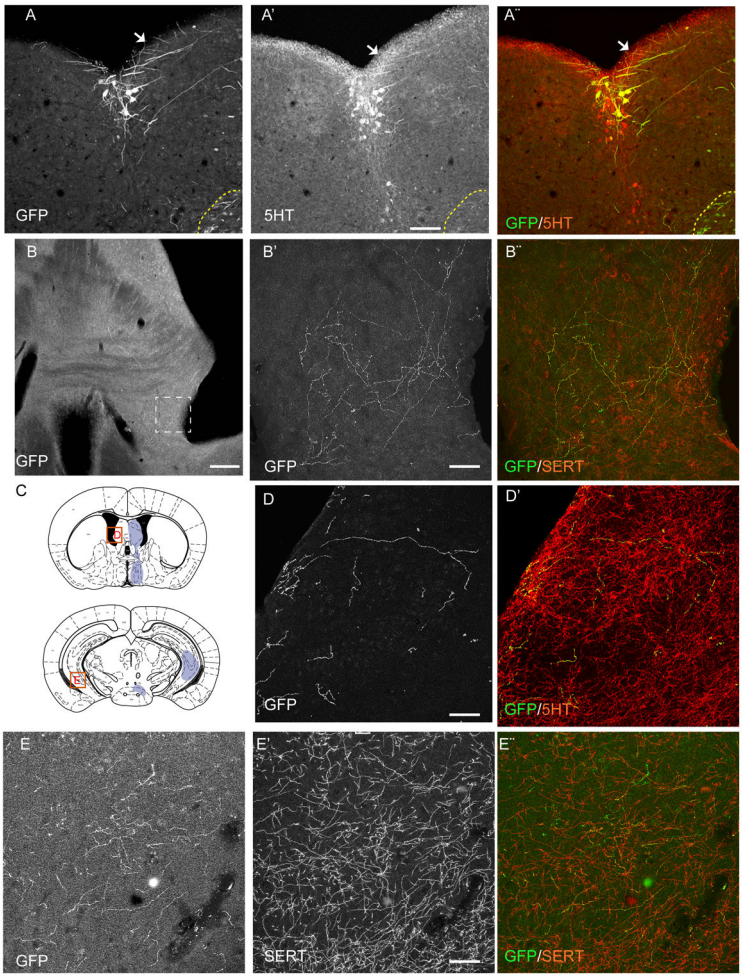

Figure 4. Anterograde tracing of serotonin neurons of the DRC

A–A″) A subset of DRN neurons, situated in the DRC, expresses GFP (A′) after injection of an AAV expressing conditionally GFP in $Sert^{Cre}$ mice. Anterogradely labeled 5-HT+ axons (arrows) are noted in the subependymal plexus of the fourth ventricle. A small number of ventrolaterally displaced cells are visibly labeled near the viral injection site (region surrounded by yellow dotted line). B–B″) B shows a low power magnification of GFP+ axon terminals abutting the lateral ventricle, B′,B″ are higher magnifications of the boxed area in B, to show the GFP-5-HT co-labeling. C) Schematic illustration showing, with purple shading, the main areas covered by the anterogradely labeled axons from B6. The red squares indicate the regions where micrographs were taken to illustrated panels D and E. D,D′) High power of GFP+/5HT+ axons in the lateral septum and the subependymal plexus. E–E″) anterogradely labeled GFP+/5HT+ axons in the ventral hippocampus. Scale bars = 200 μm in A, B. Scale bars = 20 μm in B′, B″, D–D″, and E–E″.

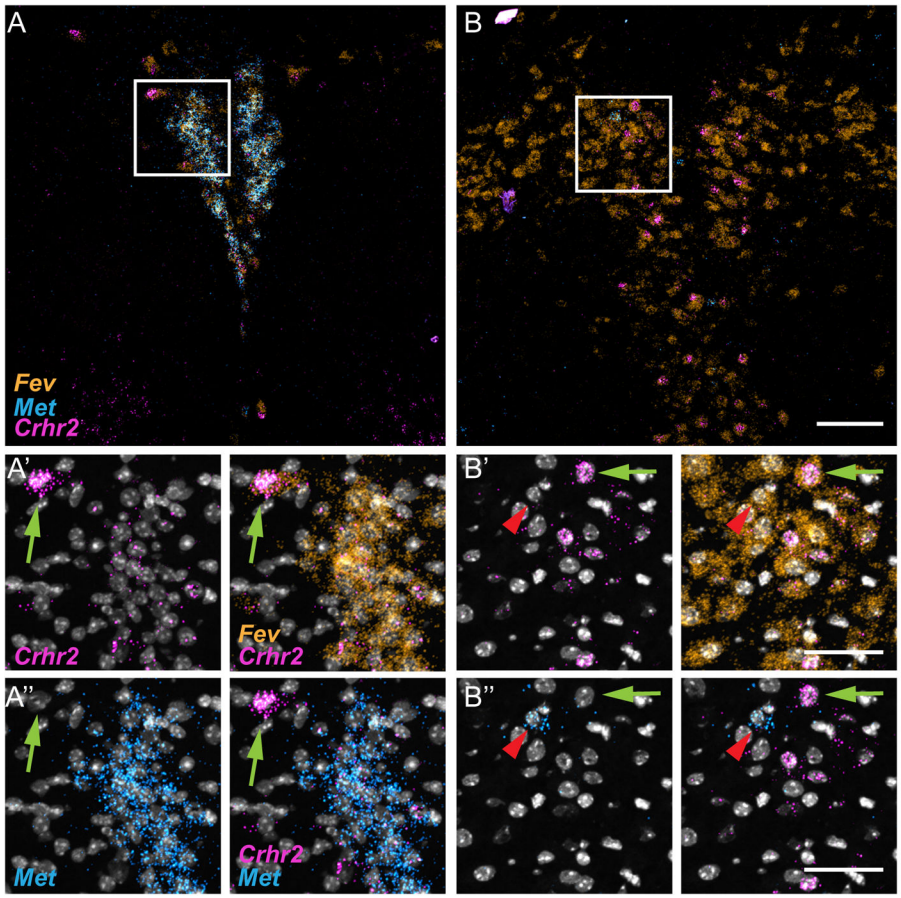

Figure 5. *Crhr2* is expressed by subsets of 5-HT neurons in the DRC

A) Coronal section through the DRC and DRI (Bregma level −5.0 mm) of the P14 mouse brain with ML-FISH performed with RNAscope probes directed toward *Fev* (orange), *Crhr2* (Magenta) and *Met* (light blue) transcripts. A′–A″) High magnification images of the region boxed in panel A showing colocalization of *Fev, Crhr2* and *Met* in the DRC. Also, note the *Fev*-positive, *Met*-negative cell which displays intense *Crhr2*-fluorescent signal (cell is indicated by green arrow). B) Coronal section through the DRD and DRV (Bregma level −4.7 mm) with ML-FISH performed as in A–A″. B′–B″) High magnification images of region boxed in panel B showing *Crhr2*-positive cells (green arrow) in the DRD, along with a sparse *Met*-expressing neuron that does not express *Crhr2* (denoted by red arrowhead). Scale bar = 100 μm in A and B. Scale bar = 50 μm, in A′–A″ and B′–B″.

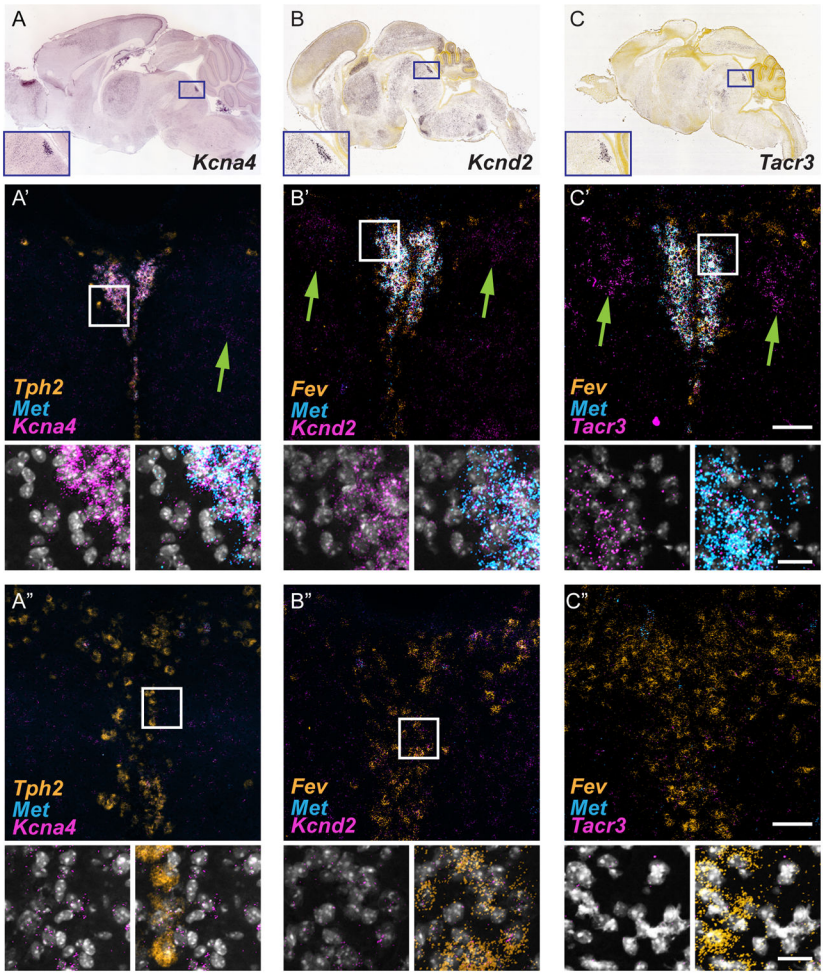

Figure 6. Genes enriched in 5-HT^{MET+} neurons in the DRC

A) *In situ* hybridization reveals *Kcna4* transcript enrichment in the DRC. Sagittal section of the adult mouse brain from the Allen Mouse Brain Atlas[43]. B) *In situ* hybridization displaying *Kcnd2* transcript enrichment in the DRC. Sagittal section of postnatal day 4 (P4) mouse brain from the Developing Mouse Brain Atlas. C) *In situ* hybridization displaying *Tacr3* transcript enrichment in the DRC. Sagittal section of P4 mouse brain from the Developing Mouse Brain Atlas. A′–C′) Coronal section through the DRC and DRI (Bregma level −5 mm) of P14 mouse brain. ML-FISH performed using RNAscope probes toward *Tph2* (orange), *Met* (light blue), and *Kcna4* (A′), *Kcnd2* (B′), or *Tacr3* (C′) (magenta); DAPI, white. Green arrows denote the expression of candidate genes by non-5-HT (*Tph2*-negative) cells surrounding the DRC. A″–C″) Coronal section through the DRD and DRV (Bregma level −4.9 mm, A″ and B″; Bregma level −4.7mm) of P14 mouse brain. ML-FISH performed as in A′, B′ and C′. Note the reduced expression of the candidate genes (magenta) in these more rostral sections. Scale bar in low mag (C′) images = 100 μm. Scale bar in high magnification insets, 25 μm.

Table 1

Genes enriched in the DRC compared to more rostral DRN

Genes with expression enriched in the DRC region as identified in the Allen Brain Atlas

Gene	Known Function
Kcna4 **	Potassium Channel
Kcnd2 **	Potassium Channel
Chrna7 *	Cholinergic receptor
Chrm2 *	Cholinergic receptor
Oprm1 *	μ-opiod Receptor
Tacr3 **	Tachykinin receptor
Cbln2	Synaptic formation
Necab2	Neuronal calcium-binding protein
Epha6	Axon guidance molecule
Lgi2	Link to epilepsy
Peg10	DNA/RNA binding protein
Zeb2	Neuronal fate
Abtb1	Translation elongation related
Cited 1	Transcription coactivator

* and ** Indicate transcripts that were chosen for further analysis by ML-FISH.

** indicates the transcripts for which ML-FISH results are shown in Figure 6